

# Hyperoxia retards growth and induces apoptosis, changes in vascular density and gene expression in transplanted gliomas in nude rats

Linda Elin Birkhaug Stuhr · A. Raa · A. M. Øyan ·  
K. H. Kalland · P. O. Sakariassen · K. Petersen ·  
R. Bjerkvig · R. K. Reed

Received: 20 February 2007 / Accepted: 1 May 2007 / Published online: 8 June 2007  
© Springer Science+Business Media B. V. 2007

**Abstract** This study describes the biological effects of hyperoxic treatment on BT4C rat glioma xenografts in vivo with special reference to tumor growth, angiogenesis, apoptosis, general morphology and gene expression parameters.

One group of tumor bearing animals was exposed to normobaric hyperoxia (1 bar,  $pO_2 = 1.0$ ) and another group was exposed to hyperbaric hyperoxia (2 bar,  $pO_2 = 2.0$ ), whereas animals housed under normal atmosphere (1 bar,  $pO_2 = 0.2$ ) served as controls. All treatments were performed at day 1, 4 and 7 for 90 min. Treatment effects were determined by assessment of tumor growth, vascular morphology (immunostaining for von Willebrand factor), apoptosis by TUNEL staining and cell proliferation by Ki67 staining. Moreover, gene expression profiles were obtained and verified by real time quantitative PCR.

Hyperoxic treatment caused a ~60% reduction in tumor growth compared to the control group after 9 days ( $p < 0.01$ ). Light microscopy showed that the tumors exposed to hyperoxia contained large “empty spaces” within the tumor mass. Moreover, hyperoxia induced a significant increase in the fraction of apoptotic cells (~21%), with no significant change in cell proliferation. After 2 bar treatment, the mean vascular density was reduced in the central parts of the tumors compared to the control and 1 bar group. The vessel diameters were significantly reduced (11–24%) in both parts of the tumor tissue. Evidence of induced cell death and reduced angiogenesis was reflected by gene expression analyses.

Increased  $pO_2$ -levels in experimental gliomas, using normobaric and moderate hyperbaric oxygen therapy, caused a significant reduction in tumor growth. This process is characterized by enhanced cell death, reduced vascular density and changes in gene expression corresponding to these effects.

**Keywords** Gliomas · Tumor growth · Angiogenesis · Apoptosis · Genes · Animal model

---

L. E. B. Stuhr (✉) · A. Raa · P. O. Sakariassen ·  
R. Bjerkvig · R. K. Reed  
Department of Biomedicine, University of Bergen, Jonas Lies  
vei 91, Bergen 5009, Norway  
e-mail: linda.stuhr@biomed.uib.no

A. M. Øyan · K. H. Kalland  
The Gade Institute, University of Bergen, Bergen, Norway

A. M. Øyan · K. H. Kalland  
Department of Microbiology and Immunology, Haukeland  
University Hospital, Bergen, Norway

K. Petersen  
Computational Biology Unit, Bergen Center for Computational  
Science, University of Bergen, Bergen, Norway

R. Bjerkvig  
NorLux Neuro-Oncology, Centre Recherche Public Santé,  
Luxembourg, Europe

## Introduction

Despite a multimodality approach including surgical resection, radiotherapy and chemotherapy, the prognosis of patients with malignant gliomas is poor with a mean survival time of 12 months. Malignant gliomas show regional differences in their vascular supply. Within the central parts, there are usually hypoxic areas caused by structural and functional vessel disturbances (perfusion- and diffusion-limited  $O_2$  delivery), while in the periphery there is usually better blood flow due to a more abundant

vasculature. While normal tissue may compensate for O<sub>2</sub> deficiency by raising the blood flow, large tumor areas lack this ability and cannot adequately counteract the restricted O<sub>2</sub> supply and therefore develop hypoxia. Thus, HbO<sub>2</sub> saturation has been shown to be significantly lower in tumors than in normal surrounding tissue with a gradual reciprocal decrease as the tumor increases in size [1, 2]. It is now widely accepted that hypoxia promotes local tumor growth, angiogenesis, invasion and reduce the effect of chemo- and radiation-therapy [3–5].

Hyperbaric oxygen treatment (HBO) will increase the oxygen tension in tumors [3, 6–9], which in turn will improve the radiation response in solid tumors [9], including gliomas [10–12] and favor normal tissue healing after radiation injury [13]. The increase in tumor pO<sub>2</sub> during and after HBO treatment is due to enhanced transport of soluble oxygen. The physically solved oxygen at normobaric air pressure is approximately 0.3 ml O<sub>2</sub>/100 ml blood with corresponding hemoglobin bound oxygen content of approximately 21 ml O<sub>2</sub>/100 ml blood. By breathing 100% oxygen at normobaric pressure, the amount of physically soluble oxygen increases to 1.8 ml O<sub>2</sub>/100 ml blood. If the atmospheric pressure is elevated to 3 bar pure oxygen, the amount of oxygen delivered to the tissue will increase to 6.0 ml O<sub>2</sub>/100 ml blood, which is sufficient to support resting tissue independent of the contribution of O<sub>2</sub> from hemoglobin [14]. When oxygen is in solution, it can reach physiologically obstructed areas not accessible to blood cells where it can provide tissue oxygenation even under conditions of impaired oxygen carriage from hemoglobin. In addition, increased arterial O<sub>2</sub>-tension, has been proposed to increase the diffusion distance sufficiently to oxygenate some of the hypoxic tumor cells [15]. In line with this, several investigators have measured a significant increase in pO<sub>2</sub> under HBO treatment on different tumors and the pO<sub>2</sub> level can be high for prolonged periods (15–60 min) post-treatment [6–8, 16].

We have in previous studies shown that it is a misconception that HBO per se will have a tumor promoting effect by increasing pO<sub>2</sub> levels that will stimulate tumor growth. For instance, we recently demonstrated a significant attenuation of mammary tumor growth after four HBO treatments (2 bar of 90 min each) [17] and four 1 and 1.5 bar hyperoxic treatments in rats [18]. Moreover, HBO treatment has been shown to have therapeutic efficacy on oral mucosal carcinomas in Syrian hamsters (2.8 bar, 30 exposures, 60 min each)[19] and on S-180 sarcomas in mice (2.5 bar, 18 exposures, 90 min each) [20]. The aim of the present study was to evaluate the effect of both normobaric (1 bar, pO<sub>2</sub> = 1.0) and hyperbaric (2 bar, pO<sub>2</sub> = 2.0) hyperoxia per se on a BT4C rat glioma xenograft model in vivo, with special reference to tumor growth, angiogenesis, apoptosis, morphology and gene expression parameters.

## Materials and methods

### Cell line

The BT4C cell line was derived from fetal rat brain cells, which were transferred to monolayer cell culture shortly after exposure to N-ethylnitrosourea in vivo [21]. The cell line is highly tumorigenic upon s.c. transplantation and has been used extensively to assess tumor growth and therapeutic effects in animal models in vivo [22–24]. The cell line was tested for mycoplasma infection by the use of Myco Alert test kit (Cambrex, USA) and then injected s.c. in the neck of two athymic nude rats (Han:rn0/rnu Rowett). When the tumors obtained a 1 cm size, the animals were sacrificed and small tumor pieces (3 mm<sup>3</sup>) were implanted s.c. in the neck of other rats for further studies.

### Animal model

A total of 24 female and male athymic nude rats (aged 6–8 weeks, weighing between 100 and 150 g) were used. The animals were bred in an isolation facility at 25°C in a specific pathogen-free environment and humidified air (55% relative humidity) on standard 12-h dark-light cycles. All animals were fed a standard laboratory diet (B & K Universal Ltd., Grimston, UK) and provided sterile water ad libitum. All procedures and experiments were approved by the Norwegian Committee for Animal Research and conducted according to the European convention for the protection of vertebrates used for scientific purposes.

### Series

The animals entered randomly into one of following three groups:

- Group 1: 21% O<sub>2</sub> (air) at 1 bar (*n* = 8)
- Group 2: 100% O<sub>2</sub> at 1 bar (*n* = 8)
- Group 3: 100% O<sub>2</sub> at 2 bar (*n* = 8)

### Pressure chamber and oxygen treatment

The animals were placed in a 130 l hyperbaric pressure chamber in clean litter-free cages (590 × 385 × 200 mm), and showered lightly with water before applying the oxygen and/if subsequently the pressure. The oxygen concentration in the pressure chamber was continuously monitored by an oxygen cell (C3, Middelsborough, England). The chamber was flushed for approximately 15 min to ensure 100% O<sub>2</sub>. In series 3, the chamber was additionally pressurized with oxygen over approximately 3 min, to 2 bar. The pressure chamber was flushed with oxygen every half hour for about 3 min to obtain an

oxygen-content above 97% at all times. The HBO treatment was given three times (day 1, 4 and 7) for 90 min each time. The temperature and humidity were held at approximately 22°C and 100%, respectively.

#### Measurement of tumor growth

Tumor size was measured externally by calipers at day 1, 4, and 8 during a short isoflurane (Shering-Plough AS, Naarum, Denmark) and N<sub>2</sub>O anesthesia (Ohmeda: BOC Health care, West Yorkshire, UK). The volume of the tumor was calculated as:  $\pi/6 \cdot (a)^2(b)$ , where a is the shortest and b is the longest transversal tumor diameter. The measurements were performed by the same person, who had no knowledge about the exposure groups.

#### Morphological analysis

The animals were sacrificed with pentobarbital (100 mg/kg) and the tumors were dissected out. One part of the tumor was fixed in 4% buffered formalin, processed and embedded in paraffin. Tissue sections of each specimen were stained using Harris Haematoxylin and Eosin (H & E, Merck, Darmstadt, Germany). The sections were analyzed with regards to apoptosis (TUNEL assay) and blood vessel density (von Willebrand factor). Indirect immunohistochemistry was performed by EnVision™ + System, horseradish peroxidase and 3′3′-diaminobenzidine (DAB) (DAKO, Glostrup, Denmark) method, as described by the manufacturer's protocol.

#### TUNEL staining

Apoptosis was assessed by the terminal transferase-mediated dUTP nick end-labeling (TUNEL) method (Boehringer Mannheim, Mannheim, Germany), performed according to the manufacturers recommendations. DNA strand breaks were labelled by attaching biotin-or digoxigenin conjugated dUTP in a reaction catalyzed by exogenous terminal deoxynucleotidyl transferase (TdT-assay) or DNA polymerase. For antigen retrieval, the slides were immersed in citrate buffer (0.1 M, pH6.0) and then microwaved for 5 min. The slides were washed in PBS before terminal deoxynucleotidyl transferase was applied to each slide and incubated for 1 h at room temperature in a humidified chamber. A stop/washing buffer was used before applying the converter POD (anti-fluorescein antibody conjugated with peroxidase as a reporter enzyme) for 30 min. Diaminobenzidine (DAB) was used as a chromogen and the slides were counterstained with hematoxylin. The density of apoptotic cells per mm<sup>2</sup> of the tumor viable zone was determined using a counter grid (10 random vision fields × 40). Apoptotic cells were expressed as a percentage of total cells.

#### Immunostaining

For detection of vascular endothelial cells we used von Willebrand factor staining. A rabbit anti-human polyclonal antibody against von Willebrand factor (DAKO, Glostrup, Denmark) was diluted in TrisBSA to a 1:250 and then 1:500 dilution. The tissue sections were incubated for 45 and 75 min, respectively, with the primary antibodies, washed three times 5 min in TBS and further incubated with anti-rabbit IgG (DAKO Cytomation Envision Kit, Labelled Polymer—HRP Anti Rabbit) for 35 min. All incubations were performed in a humidity chamber. The tissue was then washed three times in PBS. Detection was carried out using a DAB chromogen, which resulted in a positive brown staining. Harris Haematoxylin (Merck) was used for nuclear counterstaining. Negative control slides were obtained by omitting the primary antibody. For assessing cell proliferation we used an anti-rat Ki67 monoclonal antibody diluted 1:15 (Dako), and the appropriate secondary antibody, utilizing the DAKO envision kit. All sections were examined using a Nikon light microscope (THP Eclipse E600, Nikon Corporation, Tokyo, Japan) and the images were captured with a Nikon Digital Camera (DXM 1200F, Nikon Corporation, Tokyo, Japan). Image processing was performed using the LUCIA, version 4.8 (Laboratory Imaging Ltd, Prague, The Czech Republic).

Quantification of micro-vessels was performed in 10 consecutive fields, within the tumor centre as well as in the periphery. Vessel counts were averaged as the mean of 10 fields (vessels/mm<sup>2</sup>). Approximately 50 blood vessels in both the periphery and central parts of the tumor were randomly selected for diameter measurements.

#### Enzymatic modification and labelling of nucleic acid targets

cDNA for the Agilent DNA oligonucleotide microarrays was prepared from 2 µg of DNase treated total RNA using the Superscript III RT protocol as previously described [25, 26]. The T7 RNA polymerase promoter-containing double stranded cDNA was used for T7 RNA polymerase-dependent amplification of cRNA according to the Ambion T7 Megakit protocol. Aminoallyl-U (aminoallyl-UTP from Ambion) was incorporated into cRNA and crosslinked to Cy5- and Cy3-fluorochromes by means of reactive Cy-NHS compounds (Amersham). Following Qiagen RNAeasy minikit cleanup of labelling reactions, Cy5 and Cy3 incorporations were measured by absorption readings at 649 and 550 nm, respectively. Similar readings at 260 nm allowed calculation of specific labelling.

The DIG-labelled cRNA nucleic acid targets for the AB Rat Genome Survey version 1 oligonucleotide microarrays

were prepared either from 2 µg of DNase treated total RNA. The Applied Biosystems RT-IVT labelling kit supplemented with DIG-UTP (Roche Applied Science) was used according to instructions both for cDNA and cRNA synthesis. Yield and quality was checked as described above.

#### Real time quantitative PCR

Single-stranded cDNA for qPCR analysis was synthesised from 40 ng total RNA/µl using a final concentration of 5 µM random hexamer priming and M-MLV reverse transcriptase according to Ambion instructions. The qPCR volumes were 25 µl and contained 12.5 µl of 2 × Universal Master Mix, including ROX-reference dye and uracil N'-glycosylase (Applied Biosystems) and AmpliTaq Gold DNA polymerase (Perkin-Elmer), 900 nM of each primer and 250 nM of FAM-labelled TaqMan probe and 10 ng of total RNA (as hexamer primed cDNA). The mixtures were prepared in 96-well optical microtiter plates and amplified in the ABI7900HT Sequence Detection System using the following cycling parameters: 2 min at 50°C, 10 min at 95°C, and 40 alternate cycles of 15 s at 95°C and 60 s at 60°C. Dilution series of pooled samples were used for the generation of standard curves for each TaqMan assay including the endogenous control, *Actb*. Each sample cDNA was tested in triplicate. The SDS2.2 software was used for analysis and relative quantification according to program manuals and the Applied Biosystems User Bulletin #2. TaqMan real time qPCR assays (Applied Biosystems) included *Actb* (Rn00667869\_m1), *Hif1α* (Rn00577560\_m1), *Vegf* (Rn01511610\_m1), *Fgfr1* (Rn00577234\_m1), *Pdgfra* (Rn01399472\_m1) and *Amotl2* (Rn01446299\_m1).

#### Agilent DNA oligonucleotide microarrays

Approximately 500 ng of each Cy-aa-cRNA at about 100 pmoles Cy/µg aa-cRNA was first incubated with the Agilent target solution and fragmentation buffer (10 mM ZnCl<sub>2</sub>) for 30 min at 60°C (Agilent Technologies). Agilent hybridisation buffer was next added to achieve a final hybridisation volume of 490 µl for each Agilent 44 k oligonucleotide microarray (G4112A). This microarray consists of 60-mer oligonucleotides with sequences representing 41 k rat genes. Hybridisation was done at 60°C for 17 h at continuous rotation of the hybridisation chambers. The stringent wash was done in 50 ml 0.1 × SSC at 35°C for 10 min followed by three quick washes in 0.1 × SSC at room temperature followed by flushing with N<sub>2</sub> pressurized gas to remove all liquid. The oligonucleotide microarrays were scanned and features automatically extracted,

recorded and analysed using the Agilent Microarray Scanner Bundle version 7.5.1.

#### Applied biosystems rat genome survey oligonucleotide microarrays

The AB Rat Genome Survey Microarray, AB Chemiluminescence Detection Kit, AB Chemiluminescent RT-IVT Labeling Kit and AB1700 Chemiluminescent Microarray Analyzer were used as recommended. The microarray consists of 32996 60-mer oligonucleotide probes (33 k), representing 32381 curated rat genes.

#### Preprocessing: filtration and normalization of microarray data

The data files from the respective feature extraction softwares were processed using J-Express Pro v2.6 [27] (www.molmine.com) to filter and normalize the data from each hybridisation and compile gene expression profile matrix datasets for further analysis. *Agilent data filtration and normalization*: For each spot the background signals were subtracted for both channels, and low signal spots and control spots were filtered. Following this a standard global lowess normalization procedure was performed [28]. *AB data filtration and normalization*: The assay normalized intensity values were extracted per spot from the datafiles, and all flagged, weak and control spots were filtered out. Before compiled into an expression profile data matrix, the arrays were quantile normalized to be comparable [29].

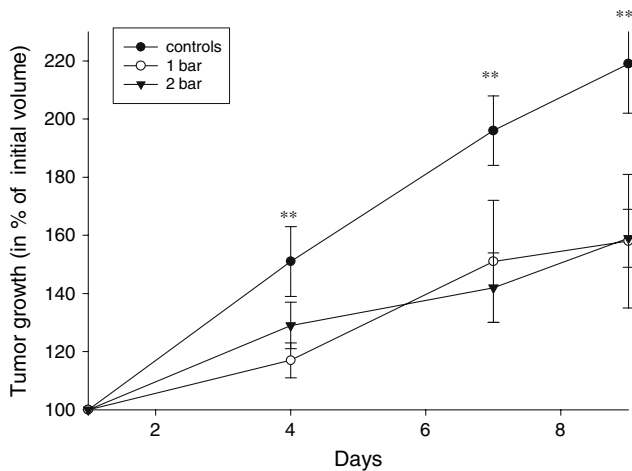
#### Statistics

Results were expressed as Means ± SD unless indicated otherwise. Differences between groups were assessed by unpaired, two-tailed Student's *t*-test or the Mann–Whitney *U* test. *p* < 0.05 was considered significant.

## Results

### Reduced tumor growth after hyperoxic treatment

About 24 tumors were studied. The tumor sizes ranged from 0.6 to 1.7 cm<sup>3</sup> prior to treatment (day1). During the observation period of 8 days, a marked increase in tumor size was seen in controls (*p* < 0.0001), whereas in both the 1 and 2 bar hyperoxic treatment groups (total 4.5 h) a ~60% reduction in growth compared to control was observed (*p* < 0.01) (Fig. 1). Interestingly, 1 and 2 bar hyperoxia resulted in a similar growth reduction.



**Fig. 1** The effect of normoxic and hyperoxic treatment on glioma growth compared to controls. Treatments were given day 1, 4 and 7 for 90 min each time. Values represent means  $\pm$  SD. Statistical significance is given as: \*\*  $p < 0.01$  controls versus each of the treated groups

Changes in tumor morphology

The BT4C tumors showed high cellularity. The cells had a pleomorphic appearance with atypical nuclei and numerous mitotic figures. The tumor vessels were irregular and showed dilatations within areas of endothelial cell proliferations (Fig. 2A). After hyperoxic treatment, numerous cells became pyknotic, indicating areas of cell death. Moreover, numerous vacuoles (“empty” spaces) as well as necrotic areas were seen within the tumors (Fig. 2B, C).

Hyperoxia does not lead to enhanced cell proliferation

We evaluated the effect of hyperoxic treatment on tumor cell proliferation using the Ki67 cell proliferation marker. Interestingly, the proportion of Ki67 positive cells were slightly less, although not statistically significant, in the

treated group compared to control (Table 1). This indicates no hyperoxia induced stimulation of cell proliferation.

Increased apoptosis in tumor cells after hyperoxic treatment

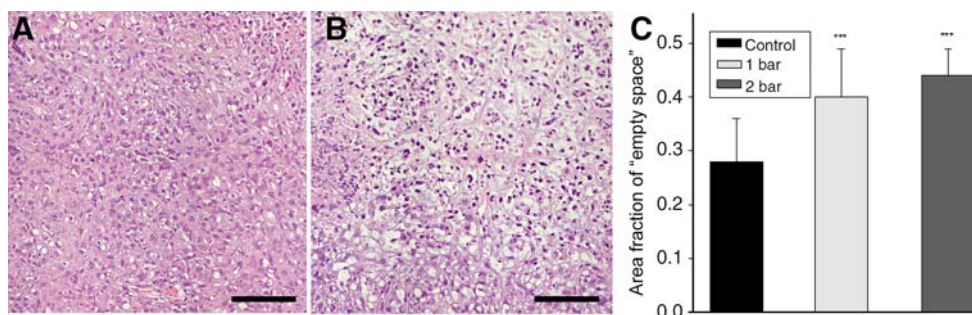
To determine whether reduction in tumor growth was related to induction of apoptosis, we performed TUNEL staining, and counted the apoptotic figures in the tumors. As shown in Table 1, a marked increase in apoptotic cells was observed after hyperoxic treatment ( $p < 0.001$ ).

Changes in mean vascular density

To determine the impact of hyperoxia on the vasculature, the vascular densities in “hot spot” areas both in the tumor centre and periphery were examined. There was a marked reduction in the mean vascular density (~50%,  $p < 0.05$ ) at 2 bar in the central parts of the tumor as demonstrated in Table 1 and Fig. 3 The diameter of the tumor vessels were significantly reduced ( $p < 0.01$ ) after hyperoxic treatment both in the central and peripheral parts of the tumor compared to controls (Table 1).

Gene expression profiling


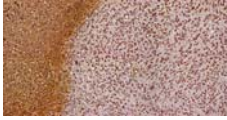

Since a reduction in tumor growth was observed, we decided to compare tumors following hyperoxic treatment with non-treated control tumors using global gene expression profiling. Two replicates using the Applied Biosystems (AB) Rat Genome Survey 33 k microarrays showed the same trend of which one is displayed in Table 2A, B (genes at least 3-fold changed). Pro-apoptotic signatures such as *GzmG* (granzyme G) and *Grid1* were induced by  $O_2$  treatment and several anti-apoptotic genes such as *Accn1*, *Nup62* and *Psen1* were suppressed. In contrast, *Snai2* (or *Snail*), the inhibitor of the classical stress induced



**Fig. 2** Eosin and hematoxylin stained tumor-tissue sections; control (A) and hypoxic treated (2 bar) (B) tumors in nude rats. The specimens were examined by using a Nikon Digital Camera DXM

1200, (Eclipse E600) at 40  $\times$  magnification (Bar = 150  $\mu$ m). The area fraction of empty space is given in C. Statistical significance is given as: \*\*\*  $p < 0.0001$  versus control

**Table 1** Mean vascular density, vascular diameter, proliferation and percentage of apoptotic cells in controls and in tumors treated with hyperoxia

	Control 1 bar, 21% O <sub>2</sub> n = 8	Test 1 bar, 100% O <sub>2</sub> n = 8	Test 2.0 bar, 100% O <sub>2</sub> n = 8
Mean vascular density (number of vessels/mm <sup>2</sup> )			
Central parts	62.1 ± 14.9	63.1 ± 16	30.3 ± 6.5*†
Periphery	24.8 ± 5.7	38.1 ± 6.1	38.5 ± 8.4
Vascular diameter (μm)			
Central parts	33.1 ± 1.4	25.2 ± 1.1**	25.2 ± 1.1 **
Periphery	37.6 ± 3.1 **	28.9 ± 1.7**	33.5 ± 4.0 **
Proliferation (% of Ki67 positive cells)	9.6 ± 1.4	8.4 ± 0.7	8.6 ± 0.6
Apoptotic cells (% of total cells)			
			
	64 ± 8.5	85 ± 5.1 ***	86 ± 4.1 ***

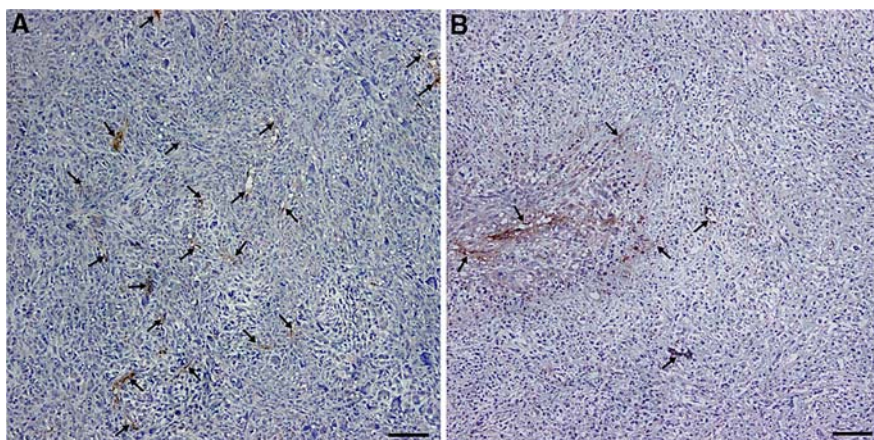
Proliferation means are given as SEM. All other values are given as Means ± SD

\*  $p < 0.02$  vs control, †  $p < 0.03$  vs 1 bar

\*\*  $p < 0.01$  vs control

\*\*\*  $p < 0.001$  vs control

**Fig. 3** Glioma tissue stained with von Willebrand factor before (A) and after hyperbaric hyperoxia (2 bar, 100% O<sub>2</sub>) (B) treatment. Blood vessels are indicated by arrows. The figures are scaled to the same magnification × 10 (Bar = 100 μm)



apoptotic pathway, was induced. The angiogenic marker *Hif2a* was several fold repressed. Also genes that control cell proliferation were differentially expressed (Table 2 and Fig. 4).

In order to achieve increased reliability of gene expressions changed less than 3-fold in treated versus non-treated samples, results based upon both Agilent 44 k and AB 33 k rat microarrays were combined (Table 3). Genes involved in angiogenesis including fibroblast growth factor receptor-1 (*Fgfr1*), vascular endothelial growth factor (*Vegf*) and platelet-derived growth factor receptor-alpha (*Pdgfra*) displayed moderate expression levels in the control tumors, but after HBO treatment over a period of 7 days their expression was clearly reduced as confirmed using real time quantitative PCR (Table 3).

## Discussion

The present study shows that both normobaric (1 bar) and hyperbaric hyperoxia (2 bar, 100% O<sub>2</sub>), three times for 90 min over a period of 8 days, reduces tumor growth, induces apoptosis and down-regulates *Vegf*, *Pdgfr-a* and *Fgfr1*.

HBO has been used in combination with both chemotherapy and radiotherapy to enhance pO<sub>2</sub> in the otherwise hypoxic tumor tissue and thereby potentiate the effect of these treatments [9]. HBO has also been used to enhance wound healing and tissue regeneration and recovery after radiation-injury. The treatment has been shown to increase blood supply to needed tissue microregions [9, 13]. However, regarding the biological effects of HBO on tumors,

**Table 2** Differentially expressed genes following hyperoxic treatment

Gene symbol	Gene name	Gene function ( <i>Rattus norvegicus</i> or <i>Homo sapiens</i> )	Fold change*
<i>A: Induced genes</i>			
Unassigned	Olfactory receptor	G protein coupled receptor protein signaling pathway	14.4
Unassigned	Homeobox distal-less DLX	DNA-binding transcription regulation, development	11.6
LOC498038	Similar to colon carcinoma related protein	Molecular function unclassified	6.3
Rap1ga17	RAP1, GTPase activating protein 1	Inhibits proliferation in keratinocytes, cell adhesion	5.5
Unassigned	Ig H VHII	B-cell- and antibody-mediated immunity	5.4
Unassigned	Ubiquitin 4	Ribosomal protein involved in proteolysis	4.7
Unassigned	Ig KAPPA LIGHT CHAIN V-I	B-cell- and antibody-mediated immunity	4.6
Unassigned	Acetyltransferase	Transferase activity	4.2
granzyme G	GzmG	Serine protease, apoptosis signaling pathway	4.2
Mcoln2	Mucolipin-2	Cation channel transport	4.0
Unassigned	Cytochrome B5 mitochondrial	Electron transport	3.8
Unassigned	Small inducible cytokine A	Pro-inflammatory chemokine	3.6
Nfatc2	Predicted nuclear factor of activated T-cells	Mesoderm development, Wnt5signaling pathway	3.6
Unassigned	Ig Kappa L V-I	B-cell- and antibody-mediated immunity	3.4
Grid1	Glutamate receptor, ionotropic, delta 1	Neurotransmitter, involved in autophagy, cell death	3.3
Unassigned	KRAB box transcription factor	Krueppel associated box, transcription factor	3.2
Ceacam1	CEA-related cell adhesion molecule 1	Arrangement of tissue structure, angiogenesis, apoptosis, tumor suppression, developmental process, regulator of integrin function	3.2
cd6 antigen	T-cell differentiation antigen CD6 precursor	Cell adhesion-mediated signaling, T-cell mediated immunity	3.2
Snai2	Snail homolog 2 ( <i>Drosophila</i> )	Neural crest transcription factor Slug, early development, Repress E-Cadherin, anti-apoptotic	3.1
<i>B: Repressed genes</i>			
RGD1559927	Predicted similar to H6 homeobox 3	DNA-binding transcription factor, development	26.1
Unassigned	Guanylate cyclase activating protein 2	G-protein mediated signaling, Calmodulin related protein	15.7
Zfp192	Predicted zinc finger protein 192	DNA-binding KRAB box transcription factor, ubiquitously expressed	13.9
Csta	Predicted cystatin A	Cysteine protease inhibitor, epidermal development and maintenance Cathepsin inhibitor	12.2
Grm5	Glutamate receptor, metabotropic 5	G protein coupled receptor, phospholipase C activating	12.1
Acs11	Acyl-CoA synthetase long-chain family member 1	Metabolism	11.8
RGD1309873	Predicted similar to hypothetical protein BC010003	Unknown function	10.6
Accn1	Amiloride-sensitive cation channel 1 neuronal	CNS Development, negative regulation of apoptosis	10.3
Unassigned	Monocarboxylic acid transporter	Cation transporter	10.2
Cldn14	Claudin 14	Cell adhesion molecule (CAM), Tight junction	7.8
Acdc	Adipocyte complement related protein of 30 kDa	Glucose metabolism, positive regulation of NF-K cascade	7.8
Ptger2	Prostaglandin E receptor 2, subtype EP2	G-protein coupled receptor, skeletal development	7.8
Hif2a	Epas1 endothelial PAS domain protein 1	Angiogenesis, differentiation	7.4

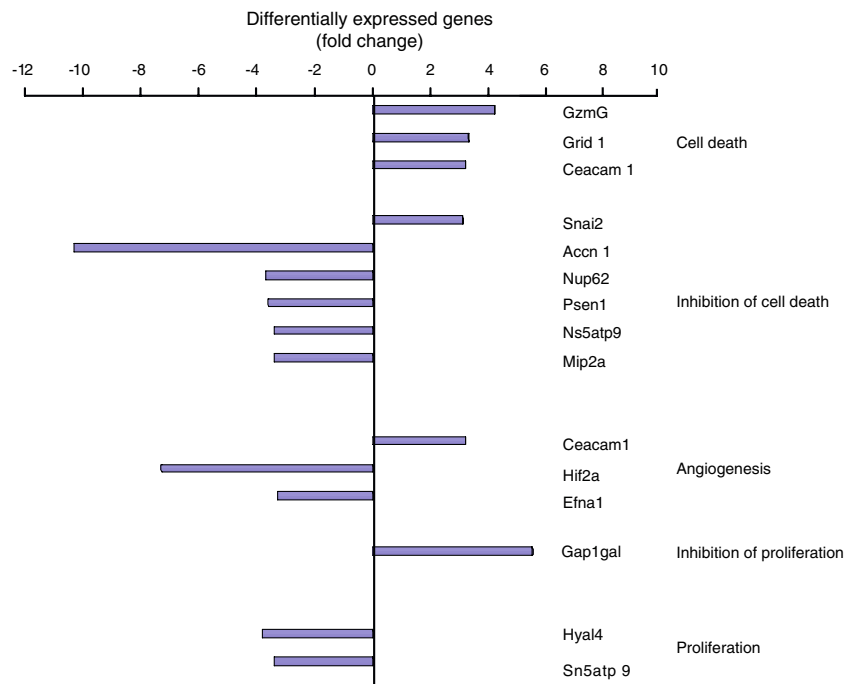
**Table 2** continued

Gene symbol	Gene name	Gene function ( <i>Rattus norvegicus</i> or <i>Homo sapiens</i> )	Fold change*
RGD1564737		Unknown function	6.8
Unassigned	Transmembrane 9 superfamily member 3	Transporter activity	6.8
Es2	Esterase 2 member of carboxylesterase-cluster 1	Detoxification	6.7
RGD1559613		Unknown function	6.6
RGD1565866	Predicted similar to FLJ44112 protein	Unknown function	6.5
Pmch	Pro-melanin-concentrating hormone	Neuropeptide signalling pathway	6.0
Unassigned	Endonuclease	DNA recombination	5.8
Cdh26	Predicted cadherin-like 26	Cell adhesion	5.7
Dpys	Dihydropyrimidinase	Nucleic acid metabolism and response to toxin	5.4
RGD1562396	Similar to bromodomain containing 8 isoform 2	Chromatin modification and regulation of cell growth	5.2
Unassigned	SET domain protein	Methyltransferase, chromatin remodulation and packaging	5.2
Mal2	T-cell differentiation protein 2	Transport activity of membrane proteins to the apical surface of the cell	5.1
Sh3g13	SH3-domain GRB2-like 3	CNS development	4.9
RGD1561830	Similar to hypothetical protein FLJ25333	Unknown	4.9
RGD1560059	Predicted to be Zgc:92710	Similar to <i>Homo sapiens</i> tight junction molecules	4.9
Arl4a	ADP-ribosylation factor-like 4A	Small GTPase	4.7
Rem2	Rad and gem related GTP binding protein 2	Small GTPase, regulation of transcription	4.7
Unassigned	Similar to factor for adipocyte differentiation 104	Differentiation	4.3
Unassigned	Similar to chaperonin heat shock 60 kDa	Protein complex assembly	4.2
Arrdc3	Arrestin domain containing 3	Unknown	4.1
Unassigned	Similar to mast cell tryptase	Serine protease	4.1
RGD1308215	Similar to hypothetical protein DKFZp434I2117	Similar to <i>Homo sapiens</i> actin binding protein, membrane protein expressed in epithelial-like lung adenocarcinoma	3.9
Hyal4	Similar to hyaluronidase 4	Carbohydrat metabolism, proliferation, migration and differentiation	3.8
Nup62	Similar to Nuclear pore glycoprotein p62/NUP62	Chromatin binding, regulation of Ras, negative regulation of cell death	3.7
RGD1560769	Similar to zinc finger protein 610	Regulation of transcription	3.6
Psen1	Presenilin 1	Notch receptor activation, activation of Wnt, negative regulation of rat neuron apoptosis, development, cell renewal	3.6
Mip2a	Similar to MBP-1 interacting protein-2A (MIP-2A)	MBP1-mediated transcriptional repression and antagonizes MBP1-mediated cell death	3.4
Msn	Moesin	Actin binding, focal adhesion assembly	3.4
Ns5atp9	NS5A (hepatitis C virus) transactivated protein 9	<i>Homo sapiens</i> PCNA associated protein, proliferation, embryogenesis, apoptosis	3.4
Lhx9	LIM/homeobox protein	Homeodomain transcription factor, neuronal differentiation	3.3
Efna1	Ephrin A1	Angiogenesis, neuron differentiation	3.3
Unassigned	Similar to RAB43, member RAS oncogene family	Small GTPase, Receptor mediated endocytosis	3.2
Unassigned	Similar to desmoglein 3	Calcium dependent cell-adhesion, regulation of epidermal differentiation	3.0

\* Parallel treated and untreated tissues were analysed using the AB 33 k rat microarrays. The J-express fold change viewer module found 117 annotated genes that were at least 3-fold differentially expressed following hyperoxic treatment (1 bar O<sub>2</sub>). In addition 52 genes with more than 3-fold change but no annotation are not shown



**Fig. 4** Differential gene expression (fold change) of samples treated with 1 bar O<sub>2</sub> compared to untreated controls is indicated on the horizontal axis. Positive fold change corresponds to up-regulated genes in the O<sub>2</sub> treated samples. Parallell treated and untreated tissues were analysed using the AB 33 k microarray. Gene symbols and functional GO terms are given in the columns to the right



**Table 3** Hyperoxic treatment and signatures influencing angiogenesis

Gene	Repression of genes (Fold change)	
	*DNA microarray	QPCR
Pdgfra	-1.5	-2.9
Fgfr1	-1.7	-7.2
Vegf	-1.8	-2

The table indicates repression of genes (fold change) as a result of treatment with 1 bar O<sub>2</sub> compared to the control

\* Fold changes represent the average values of Agilent 44 k microarrays (one replicate, dye swap) and AB 33 k microarrays (two replicates)

the therapeutic implications may be more complex. On the one hand, HBO treatment may recruit hypoxic tumor cells into the pool of proliferative cells. This should in turn lead to enhanced tumor growth and eventually increased neo-vascularization. On the other hand, tumor cells may, compared to normal cells, be quite sensitive to increased oxygen tensions. The current work supports previous conclusions from our group demonstrating that hyperoxic treatment has a significant inhibitory effect on the growth of mammary tumors [17, 18]. Also, mouse MT-7 mammary carcinoma xenografts showed a reduced number of metastatic lung colonies after 3 weeks of exposure to 70% O<sub>2</sub> [30, 31]. Some cell lines have, however, been shown to be oxygen resistant [30] indicating a variability in O<sub>2</sub> sensitivity between different kinds of tumor cells. The effect of hyperoxia may also depend of several factors

including tumor stage, size or the duration O<sub>2</sub> exposure. The tumors that showed growth inhibition displayed abundant morphology changes. Most pronounced were the vacuoles and empty spaces in the tumor tissue (Fig. 2B), which corresponds to what is found in mammary tumors after similar treatments [18].

We observed an induction of apoptosis as indicated by elevated number of tunnel-positive apoptotic tumor cells (~20%). This corresponds well with previous findings showing a ~25% increase in apoptosis found in DMBA induced mammary rat tumors treated with 1 and 1.5 bar pure oxygen [18]. In the current study, we did not observe any damage of normal tissue after HBO treatment; not even in the lungs, which are known to be sensitive to HBO exposure [32]. The gene expression arrays showed an increased expression of genes known to induce cell death as well as a reduced expression in genes known to inhibit cell death. The inhibition of tumor growth is therefore most likely induced by activation of specific genes involved in cell death programs (Fig. 4).

Hyperoxic treatment showed a slight but insignificant decrease in tumor cell proliferation. Our gene expression data indicate a reduction in cell proliferation after hyperoxic treatment (Fig. 4). Other reports have shown reduced cell proliferation after HBO exposure, suggesting treatment effects on cell-cycle regulatory mechanisms [33, 34]. Thus, it may take more than three hyperoxic treatments to induce a reduction in cell proliferation.

Hypoxia induces the formation of new tumor blood vessels necessary for further tumor growth [35]. One might

therefore expect that hyperoxia may remove the stimulus for the angiogenic switch. Normally, hyperoxic treatment is known to increase vessel development in normal tissue and in wound healing. Interestingly, the present study demonstrated that hyperoxia reduced the vascular density in central parts of the gliomas. This also support findings seen in mammary tumors exposed to hyperoxia [18]. However, no change in MVD was found after normoxic hyperoxia. Since hyperbaric hyperoxia induces a higher  $pO_2$  in the tumor tissue than 1 bar hyperoxia, this can indicate that gliomas needs a certain  $pO_2$  level to influence the angiogenesis. Our results indicate a decrease in vascular diameters both in the periphery and central parts of the tumor. This may be expected since hyperoxia is known to induce vasoconstriction [14]. Vasoconstriction may lead to inadequate blood supply and lack of metabolic exchange resulting in tumor necrosis and regression [36].

In our PCR verified gene expression study three genes involved in angiogenesis and tumor growth were significantly downregulated; *Pdgfra*, *Fgfr1* and *Vegf*.

Gliomas show high expression levels of *Pdgf* which may stimulate both tumor and endothelial cell proliferation [37]. *Pdgfra* (receptor  $-\alpha$ ) binds *Pdgf* with high specificity and inhibition of this epitope has been shown to inhibit tumor growth [38–40].

The expression of *Fgfr1* mRNA in astrocytomas increases as malignancy progresses and it has been shown that *Fgfr1* inhibition may lead to decreased tumor growth in glioma cell lines [41, 42].

Many tumor models have demonstrated a close relationship between local oxygen deficiency and the production of Hif-1 $\alpha$  and Vegf [43, 44]. Hif-1 $\alpha$  activity as well as Vegf secretion is tightly regulated by the oxygen-level, and in the well oxygenated state they are rapidly degraded [45]. Thus, by reoxygenating the tumor tissue with normobaric and hyperbaric oxygen it is reasonable to assume that both Hif1 $\alpha$  and Vegf could have been down-regulated. This would indirectly prevent angiogenesis and thereby also tumor growth. The reduction in *Vegf* found after hyperoxic treatment in the present study supports this notion.

The significant down-regulation of *Pdgfra*, *Fgfr1* and *Vegf* after hyperoxic treatment per se can at least partly explain the observed inhibition in tumor growth.

The mechanism(s) by which hyperoxia influence(s) tumor growth is currently not known. However, it should be emphasized that both normobaric and hyperbaric hyperoxia may free oxygen radicals (ROS). ROS activity is known to be elevated during hyperoxia [46, 47]. When the level of free oxygen radical production exceeds endogenous cellular antioxidant capacity it can create an “oxidative stress” which can lead to cell death [48]. Free oxygen radicals have previously been shown to induce apoptosis and also inhibit angiogenesis [49]. In the literature it seems as if

ROS activity may have “two faces”. It appears as though the action of free radicals on normal and tumor cells are diametrically opposite. When free radicals attack normal cells, DNA damage can occur, leading to development of tumors, whereas ROS in tumor cells has an unexpected but highly beneficial action, namely inhibition of tumor cells (review: 49). Since superoxide dismutase (SOD) activity in most tumors has been shown to be lower than in normal tissue, this might make the tumors even more susceptible to increased ROS activity during hyperoxic exposure. HBO may increase intratumoral ROS levels past the threshold and induce tumor cell destruction, as has been shown in vitro in mouse fibroblast cells [50] and in vivo in mice with S-180 sarcoma [21]. So an increase in ROS activity by HBO might be beneficial in tumors.

In conclusion, we show that both normobaric (1 bar,  $pO_2 = 1.0$ ) and hyperbaric hyperoxia (2 bar,  $pO_2 = 2.0$ ) significantly *inhibit* tumor growth in transplanted gliomas in nude rats after only three hyperoxic exposures (or a total of 4.5 h of treatment). Since HBO greatly improves oxygen perfusion in tumors it alters the hypoxic microenvironment. Thus, hyperoxia did affect the tumors by inducing cell death and by reducing the vascular density in the central parts of the tumor. These processes were characterized by a down-regulation of genes known to have implications in tumor growth and neo-vascularization. Further studies should be aimed at elucidating the hyperoxic effect on gliomas and also combining hyperoxic treatment with both new and conventional treatment methods.

**Acknowledgement** We would like to thank Harald Sundland at NUI, Bergen, for assistance with the pressure chamber and technical assistance by Tore Jacob Raa at Gades Institute, Department of pathology, Haukeland University Hospital, Bergen, Norway. Per Øyvind Enger, Department of Biomedicine, are gratefully acknowledged for morphology assistance. We thank Sue Olsen for real time qPCR and Hua My Hoang for the DNA microarray work. This study was supported by the Norwegian Cancer Society, the Research Council of Norway, Innovest AS, Helse-Vest, Haukeland University Hospital, The Bergen Translational Research program, The Centre Recherche de Public Sante’ Luxemburg, and the European Commission 6th Framework Program Contract 504742.

## References

1. Vaupel P, Kallinowski F, Okunieff P (1989) Blood flow, oxygen and nutrient supply, and metabolic microenvironment of human tumors: a review. *Cancer Res* 1:6449–6465 (Review)
2. Höckel M, Vaupel P (2001) Tumor hypoxia: definitions and current clinical, biologic, and molecular aspects. *J Natl Cancer Inst* 21:266–276 (Review)
3. Brizel DM, Lin S, Johnson JL, Brooks J, Dewhirst MW, Piantadosi CA (1995) The mechanisms by which hyperbaric oxygen and carbogen improve tumor oxygenation. *Br J Cancer* 72:1120–1124
4. Semenza GL (2000) HIF-1 and human disease: one highly involved factor. *Genes Dev* 15:1983–1991 (Review)

5. Helczynska K, Kronblad A, Jogi A, Nilsson E, Beckman S, Landberg G, Pahlman S (2003) Hypoxia promotes a dedifferentiated phenotype in ductal breast carcinoma in situ. *Cancer Res* 1:1441–1444
6. Beppu T, Kamada K, Yoshida Y, Arai H, Ogasawara K, Ogawa A (2002) Change of oxygen pressure in glioblastoma tissue under various conditions. *J Neurooncol* 58:47–52
7. Becker A, Kuhnt T, Liedtke H, Krivokuca A, Bloching M, Dunst J (2002) Oxygenation measurements in head and neck cancers during hyperbaric oxygenation. *Strahlenther Onkol* 178:105–108
8. Kinoshita Y, Kohshi K, Kunugita N, Tosakki T, Yokota A (2000) Preservation of tumor oxygen after hyperbaric oxygenation monitored by magnetic resonance imaging. *Br J Cancer* 82:88–92
9. Al-Waili NS, Butler GJ, Beale J, Hamilton RW, Lee BY, Lucas P (2005) Hyperbaric oxygen and malignancies: a potential role in radiotherapy, chemotherapy, tumor surgery and phototherapy. *Med Sci Monit* 11:279–289
10. Kohshi K, Kinoshita Y, Imada H, Kunugita N, Abe H, Terashima H, Tokui N, Vemura S (1999) Effects of radiotherapy after hyperbaric oxygenation on malignant gliomas. *Br J Cancer* 80:236–241
11. Ogawa K, Yoshii Y, Inoue O, Toita T, Saito A, Kakinohana Y, Adachi G, Ishikawa Y, Kin S, Murayama S (2003) Prospective trial of radiotherapy after hyperbaric oxygenation with chemotherapy for high-grade gliomas. *Radiother Oncol* 67:63–67
12. Ogawa K, Yoshii Y, Inoue O, Toita T, Saito A, Kakinohana Y, Adachi G, Iraha S, Tamaki W, Sugimoto K, Hyodo A, Murayama S (2006) Phase II trial of radiotherapy after hyperbaric oxygenation with chemotherapy for high-grade gliomas. *Br J Cancer* 9:862–868
13. Feldmeier JJ, Hampson NB (2002) A systemic review of the literature reporting the application of hyperbaric oxygen prevention and treatment of delayed radiation injury: an evidence-based approach. *Undersa Hyperbar Med* 29:4–30
14. Gill AL, Bell CAN (2004) Hyperbaric oxygen: its uses, mechanisms of action and outcomes. *Q J Med* 97:385–395
15. Siemann DW, Warrington KH, Horsman MR (2000) Targeting tumor blood vessels: an adjuvant strategy for radiation therapy. *Radiother Oncol* 57:5–12 (Review)
16. Jamieson D, van den Bronk HAS (1963) Measurements of oxygen tension in cerebral tissues of rats exposed to high pressure of oxygen. *J Appl Physiol* 18:869–876
17. Stuhr LE, Iversen VV, Straume O, Maehle BO, Reed RK (2004) Hyperbaric oxygen alone or combined with 5-FU attenuates growth of DMBA-induced rat mammary tumors. *Cancer Lett* 210:35–40
18. Raa A, Stansberg C, Steen VM, Bjerkvig R, Reed RK, Stuhr LEB (2007) Hyperoxia retards growth and induces apoptosis and loss of glands and blood vessels in DMBA-induced rat mammary tumors. *BMC Cancer* 7:23 (Epub ahead of print)
19. McDonald KR (1996) Effect of hyperbaric oxygenation on existing oral mucosal carcinoma. *Laryngoscope* 106:957–959
20. Lian QL (1995) Effects of hyperbaric oxygen on S-180 sarcoma in mice. *Undersea Hyperbar med* 22:153–160
21. Laerum OD, Rajewsky MF, Schachner M, Stavrou D, Haglid KH, Haugen Å (1977) Phenotypic properties of neoplastic cell lines developed from fetal rat brain cells in culture after exposure to ethylnitrosourea in vivo. *Z. Krebsforsch* 89:273–295
22. Sandstrom M, Johansson M, Andersson U, Bergh A, Bergenheim AT, Henriksson R (2004) Related Articles, Links The tyrosine kinase inhibitor ZD6474 inhibits tumor growth in an intracerebral rat glioma model. *Br J Cancer* 91:1174–1180
23. Thorsen F, Ersland L, Nordli H, Enger PO, Huszthy PC, Lundervold A, Standnes T, Bjerkvig R, Lund-Johansen M (2003) Imaging of experimental rat gliomas using a clinical MR scanner. *J Neurooncol* 63:225–231
24. Vallbo C, Bergenheim T, Hedman H, Henriksson R (2002) The antimicrotubule drug estramustine but not irradiation induces apoptosis in malignant glioma involving AKT and caspase pathways. *J Neurooncol* 56:143–148
25. Rostad K, Mannelqvist M, Halvorsen OJ, Oyan AM, Bo TH, Stordrange L, Olsen S, Haukaas SA, Lin B, Hood L, Jonassen I, Akslen LA, Kalland KH (2007) ERG upregulation and related ETS transcription factors in prostate cancer. *Int J Oncol* 30:19–32
26. Anensen N, Oyan AM, Bourdon JC, Kalland KH, Bruserud O, Gjertsen BT (2006) A distinct p53 protein isoform signature reflects the onset of induction chemotherapy for acute myeloid leukemia. *Clin Cancer Res* 12:3985–3992
27. Dysvik B, Jonassen I (2001) J-Express: exploring gene expression data with Java. *Bioinformatics* 17:369–370
28. Yang YH, Buckley MJ, Speed TP (2001) Analysis of cDNA microarray images. *Briefings in Bioinformatics* 2:341–349
29. Bolstad BM, Irizarry RA, Astrand M, Speed TP (2003) A comparison of normalization methods for high density oligonucleotide array data based on variance and bias. *Bioinformatics* 19:185–193
30. Margaretten NC, Witschi H (1988) Effects of hyperoxia on growth characteristics of metastatic murine tumors in the lung. *Cancer Res* 15:2779–2783
31. Lindenschmidt RC, Margaretten N, Griesemer RA, Witschi HP (1986) Modification of lung tumor growth by hyperoxia. *Carcinogenesis* 7:1581–1586
32. Clark JM (1993) Oxygen toxicity. In: Bennet P, Elliot D (eds) *The physiology and medicine of diving*, 4th edn. WB Saunders Company Ltd, 121–169
33. McMillan T, Calhoun KH, Mader JT, Stiernberg CM, Rajaraman S (1989) The effect of hyperbaric oxygen on oral mucosal carcinoma. *Laryngoscop* 99:241–244
34. Daruwalla J, Christophi C (2006) Hyperbaric oxygen therapy for malignancy: a review. *World J Surg*, e-publish ahead of print nov 7
35. Folkman J (1995) Clinical application of research on angiogenesis. *N Engl J Med* 333:1757–1763
36. Hanahan D, Folkman J (1996) Patterns and emerging mechanisms of the angiogenic switch during tumorigenesis. *Cell* 86:353–364
37. Shih AH, Holland EC (2006) Platelet-derived growth factor (PDGF) and glial tumorigenesis. *Cancer Lett* 232:139–147
38. Ko YJ, Small EJ, Kabbinnar F, Chachoua A, Taneja S, Reese D, DePaoli A, Hannah A, Balk SP, Bublej GJ (2001) A multi-institutional phase II study of SU101, a platelet-derived growth factor receptor inhibitor, for patients with hormone-refractory prostate cancer. *Clin Cancer Res* 7:800–805
39. Eckhardt SG, Rizzo J, Sweeney KR, Cropp G, Baker SD, Kraynak MA, Kuhn JG, Villalona-Calero MA, Hammond L, Weiss G, Thurman A, Smith L, Drengler R, Eckardt JR, Moczygemba J, Hannah AL, Von Hoff DD, Rowinsky EK (1999) Phase I and pharmacologic study of the tyrosine kinase inhibitor SU101 in patients with advanced solid tumors. *J Clin Oncol* 17:1095–1104
40. Sulzbacher I, Birner P, Traxler M, Marberger M, Haitel A (2003) Expression of platelet-derived growth factor- $\alpha$  is associated with tumor progression in clear cell renal cell carcinoma. *Am J Clin Pathol* 120:107–112
41. Bian XW, Du LL, Shi JQ, Cheng YS, Liu FX (2004) Correlation of bFGF, FGFR1 and VEGF expression with vascularity and malignancy of human astrocytomas. *Anal Quant Cytol Histol* 22:267–274
42. Yamada SM, Yamaguchi F, Brown R, Berger MS, Morrison RS (1999) Suppression of glioblastoma cell growth following anti-sense oligonucleotide-mediated inhibition of fibroblast growth factor receptor expression. *Glia* 28:66–76

43. Maxwell PH, Dachs GU, Gleadle JM, Nicholls LG, Harris AL, Stratford IJ, Hankinson O, Pugh CW, Ratcliffe PJ (1997) Hypoxia-inducible factor-1 modulates gene expression in solid tumors and influences both angiogenesis and tumor growth. *Proc Natl Acad Sci* 94:8104–8109
44. Thews O, Wolloscheck T, Dillenburg W, Kraus S, Kelleher DK, Konecny MA, Vaupel P (2004) Microenvironmental adaptation of experimental tumors to chronic vs acute hypoxia. *Br J cancer* 13:1181–1189
45. Marxsen JH, Schmitt O, Metzen E, Jelkmann W, Hellwig-Burgel T (2001) Vascular endothelial growth factor gene expression in the human breast cancer cell line MX-1 is controlled by the O<sub>2</sub> availability in vitro and in vivo. *Ann Anat* 183:243–249
46. Yamaguchi KT, Stewart RJ, Wang HM, Hudson SE, Vierra M, Akhtar A et al (1992) *Free Radic Res Commun* 16:167–174
47. Narkowicz CH, Vial JH, McCartney P (1993) Hyperbaric oxygen therapy increases free radical levels in the blood of humans. *Free Radical Res Comm* 19:71–80
48. Halliwell B, Gutteridge JM (1990) Role of free radicals and catalytic metal ions in human disease: an overview. *Methods Enzymol* 186:1–85
49. Das UN (2002) A radical approach to cancer. *Med Sci Monit* 8:79–92
50. Conconi MT (2003) Effects of hyperbaric oxygen on proliferative and apoptotic activities and reactive oxygen species generation in mouse fibroblast 3T3/J2 cell line. *J Invest Med* 51:227–232